



---

## Photocatalytic Activity of Lanthanum Nickelate under Simulated Visible-Light Irradiation

Kim-Ngan Huynh, Kieu Oanh Pham, Manh-Thang Ngo, Minh-Vien Le\*

Department of Inorganic Chemical Engineering, Ho Chi Minh City University of Technology, Ho Chi Minh City 70000, Vietnam

---

**Abstract** Crystalline perovskite typed  $\text{LaNiO}_3$  was synthesized by the sol-gel method and characterized by X-ray diffraction XRD, thermogravimetric analysis TG/DTA, scanning electron microscope SEM, and specific surface area BET. Photocatalytic activities of the “as-synthesized”  $\text{LaNiO}_3$  under simulated visible lights were accessed through removal of 2-naphthol residues in aqueous solutions. The characteristics and consequently photocatalytic activities of the “as-synthesized”  $\text{LaNiO}_3$  are strongly affected by calcination temperature and – time, with the best results obtained at 700°C and 3 hours, respectively. The FT-IR spectra revealed that parts of 2-naphthol and/or its photocatalytic transformation products remained on the catalysts’ surface. However, these catalysts could be re-used up to 3-times with slightly decreasing 2-naphthol removal yields. Besides, the kinetics of 2-naphthol removal was found to be of pseudo-first order reactions.

**Keywords**  $\text{LaNiO}_3$ , Photocatalytic Activity, 2-naphthol

---

### Introduction

Due to the increasing environmental pollution and energy shortage, efforts have been focused on the development of photocatalysts which could effectively remove organic pollutants in wastewater under solar lights [1]. For this purpose, mixed metal oxides with general formula  $\text{LaMO}_3$  – where M denotes a transition metal – belong to the most potential materials owing to their intrinsic electronic, magnetic and optic properties which provide high catalytic activities and application in many fields [2-6].

Among the  $\text{LaMO}_3$  type compounds, lanthanum nickelate ( $\text{LaNiO}_3$ ) with perovskite structure has attracted considerable attention in many applications [7]. In term of photocatalysis,  $\text{LaNiO}_3$  has shown high activities in treating organic contaminants under UV- and visible light illuminations [8].  $\text{LaNiO}_3$  powders synthesized by sol-gel method exhibited narrow band-gaps of 2.26 eV [9] or 2.28 eV [10]. These narrow band gaps could be overcome by absorbing visible lights photons, followed by generation of electron-hole pairs which contribute to the oxidative decomposition of organic compounds. It is worth to note the photocatalytic activity of  $\text{LaNiO}_3$  perovskite under visible lights is much higher compared to that of the commercial Degussa P25, enabling to remove up to 74.9 % methyl orange (MO) after 5 hours illumination [10].  $\text{LaNiO}_3$  powders synthesized by a mechano-chemical method [7] exhibited even higher effectivity enabling to remove more than 99 % MO after 2 hours illumination.  $\text{LaNiO}_3$  perovskite synthesized by a single-reverse microemulsion process [8] also showed very high photocatalytic activities towards naphthalene removal. In summary, perovskite typed  $\text{LaNiO}_3$  belongs to the most promising materials for decomposition of organic compounds under solar lights illumination and its synthesis by different methods should be further investigated.



On the other hand, phenols figure prominently in the list of priority pollutants of the US Environmental Protection Agency and the European Union [11]. The content of phenolic compounds in industrial effluents is usually high and they belong to the most harmful pollutants in natural waters [12]. Among phenolic compounds, 2-naphthol is a secondary product in many industrial fields e.g. chemical, paper, paint and pesticide production, and it is known as a hazardous substance to humans and the environment [13]. Therefore, various methods have been developed to remove and/or eliminate 2-naphthol, e.g. biodegradation [14], photodegradation using  $\text{TiO}_2$ - $\text{SiO}_2$  [15], sorption on immobilized organo-bentonite [16], catalytic wet air oxidation using  $\text{CuO}_x$  and  $\text{MnO}_x$  [12]. These methods have their intrinsic advantages and limitations. However, the photocatalytic oxidation belongs to the emerging technologies for its capability to mineralize organic micro-pollutants and/or transform them into less harmful compounds [11]. Therefore, this study aimed to synthesize  $\text{LaNiO}_3$  nanoparticles with perovskite typed structure by a sol-gel method and evaluate their photocatalytic activities for removing 2-naphthol under simulated solar lights illumination

### Experiment

All chemicals:  $\text{La}(\text{NO}_3)_3 \cdot 6\text{H}_2\text{O}$  (99%),  $\text{Ni}(\text{NO}_3)_2 \cdot 6\text{H}_2\text{O}$  (99%), citric acid ( $\text{C}_6\text{H}_8\text{O}_7 \cdot \text{H}_2\text{O}$ ) (99,9%) and 2-naphthol ( $\text{C}_{10}\text{H}_8\text{O}$ , 99,9%) were purchased from Merck and used without further purifications. De-ionized water was used for preparing solutions.

#### Synthesis of $\text{LaNiO}_3$

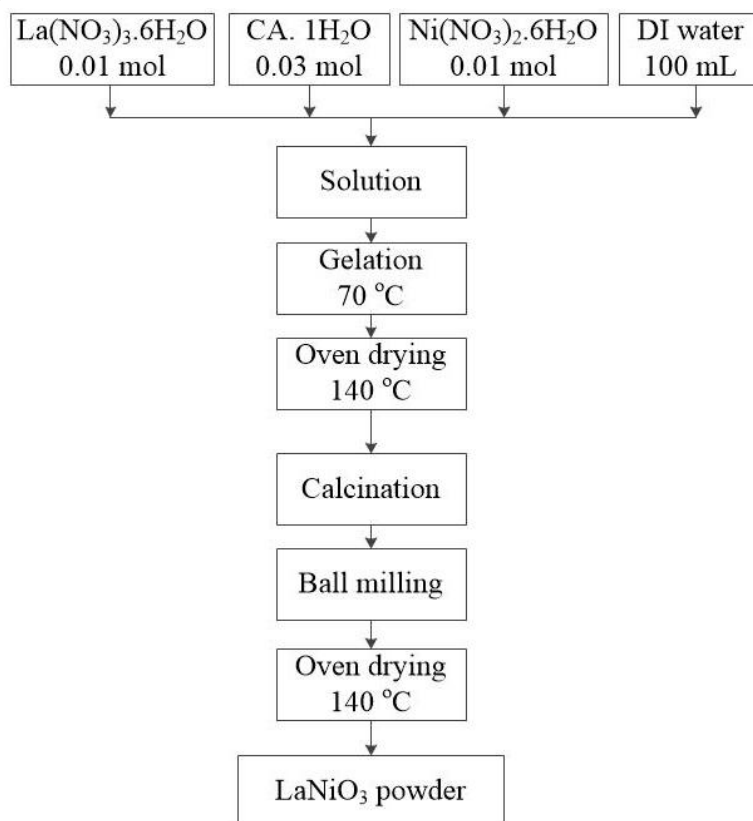


Figure 1: Schematic of perovskite  $\text{LaNiO}_3$  powder synthesis

The sol-gel method for synthesis of  $\text{LaNiO}_3$  using  $\text{La}(\text{NO}_3)_3 \cdot 6\text{H}_2\text{O}$ ,  $\text{Ni}(\text{NO}_3)_2 \cdot 6\text{H}_2\text{O}$  as precursors is schematically presented in Fig.1. Firstly, 0.01 mol  $\text{La}(\text{NO}_3)_3 \cdot 6\text{H}_2\text{O}$  and 0.01 mol  $\text{Ni}(\text{NO}_3)_2 \cdot 6\text{H}_2\text{O}$  were dissolved in 100 mL deionized water. After that, 0.03 mol citric acid was slowly added into this solution under vigorous mixing and the temperature was maintained at 80 °C to produce gels. The obtained gel was then dried at 140 °C for 2 hours to form primary powder. Finally, the primary powder was calcined under aerated conditions at 500 °C for 1 hour, ground and calcined further at different temperatures of 650, 700, 750 or 800 °C for 3 hours.



### Characterization of $\text{LaNiO}_3$

The X-ray powder diffraction (XRD) patterns of the samples were recorded using an X-ray diffractometer (D2 Phaser, Bruker) equipped with a  $\text{CuK}_\alpha$  radiation source ( $1.5418 \text{ \AA}$ ) and nickel filter. The voltage was set at 50 kV and the current was 200 mA, while the scanned  $2\theta$  range was  $15 - 70^\circ$  with a step size of  $0.02^\circ$ . The infrared (IR) spectra were collected between  $400 - 4,000 \text{ cm}^{-1}$  using a Fourier-transform infrared spectrometer, FTIR, (Digilab FTS-3500, Biorad). The IR sample was pelletized into a powdered mixture that contained 3 wt%  $\text{LaNiO}_3$  ( $700^\circ\text{C}$  calcined for 3h) and 97% KBr. The reported spectra are the average over 64 scans. The microstructure and morphology of the synthesized powder samples were characterized by scanning electron microscope SEM (FE SEM S4800, Hitachi, Japan). Specific surface area analyses of samples were measured by nitrogen adsorption-desorption isotherms at 77 K using Quantachrome NOVA 1000e. The band gap energy of samples was determined by diffuse reflectance spectra (DRS) from 300 to 800 nm, scanning step was 2 nm, at 400 nm/min speed, using Solid UV-vis JASCO Corp equipment. The simultaneous thermal analysis (TG/DSC) of the sample was performed in a Setaram Instrumentation apparatus under atmospheric pressure with heating rate  $10^\circ\text{C}/\text{min}$ .

### Photocatalytic activity test

Photocatalytic activities of the synthesized products were evaluated by examining the removal of 2-naphthol residues in water with a 26 W mercury lamp which emits in the wavelength range of 390 – 750 nm. A stock solution of 1000 ppm 2-naphthol in water was prepared and then diluted accordingly for this test. Concentrations of 2-naphthol in aqueous samples were determined by measuring absorbance at 254 nm with an UV-Vis spectrophotometer (Thermo Scientific, Evolution 60S).

The photocatalytic processes were performed as followed: 0.20 g of the synthesized products was suspended in 200 mL aqueous solutions of 2-naphthol in the dark under vigorous stirring for 60 min. This suspension was then exposed to visible lights illumination from the 26 W mercury lamp in a water-jacket pyrexphotoreactor. After periods of time, 3mL-aliquots of suspension were withdrawn, filtered through Millipore syringe filters ( $0.45 \mu\text{m}$ ), and their 2-naphthol concentration were determined.

To evaluate the reusability, the suspension after 5 h reaction was centrifuged and washed with deionized water in several times. The collected catalyst was dried in electric oven at  $120^\circ\text{C}$  for 1 h and served for the next round which was conducted in the same conditions with the first round.

## Results and Discussion

### Characteristics of the Synthesized Products

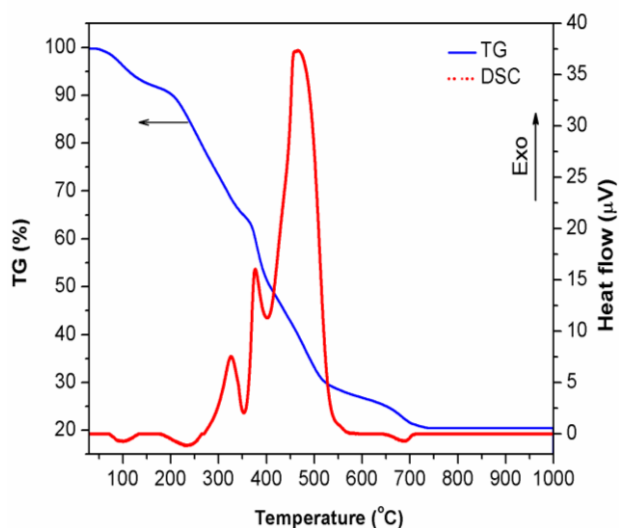


Figure 2: TG/DSC curves during heating under air of the primary powder

Details of the synthesis procedure in Fig.1 were confirmed by results of TG/DSC analysis of the primary powders and XRD analysis of the as synthesized products. Fig. 2 shows the decrease of primary powder weight



slowed down and ended at about 500 °C and 700 °C, respectively. This weight loss was due to the decomposition of citrate, carbonate and carboxylate complexes in the primary powders, which was confirmed by 3 exothermic peaks at temperatures 325 °C, 375 °C and 465 °C, respectively, in the DSC curve [2]. Besides, a small endothermic peak at 690 °C might indicate reconstructions inside the products in this elevated temperature region to establish its perovskite structure [17]. Therefore, the primary powder should be calcined at 500 °C for 1 hour to decompose all the citrate, carboxylate and carbonate complexes and then calcined further at elevated temperatures, as described in Fig. 1.

Fig.3 compares the XRD patterns of a  $\text{LaNiO}_3$  reference (JCPDS 88-0633) and synthesized products which were calcined at various temperatures. For the first glance, all the synthesized products including that one calcined at 650 °C provided well-indexed peaks as the  $\text{LaNiO}_3$  reference. This deviation from the TG/DSC results is due to the one-hour pre-calcination step at 500 °C. An increase in calcination temperature between 650 °C and 750 °C led to higher  $\text{LaNiO}_3$  perovskite peaks, indicating higher crystallinity degrees. However, traces of NiO impurities already appeared as consequences of the  $\text{LaNiO}_3$  decomposition at calcinations temperature 750 °C [17], which became more severe at 800 °C when the characteristic perovskite peaks decreased. In addition, the specific surface areas of products decreased from 9.1  $\text{m}^2/\text{g}$  to 7.5  $\text{m}^2/\text{g}$  when the calcinations temperature increased from 700 °C to 750 °C, respectively. As too low specific surface areas might negatively affect the photocatalytic activities of synthesized products, 700 °C was chosen as calcinations temperature in our synthesis procedure.

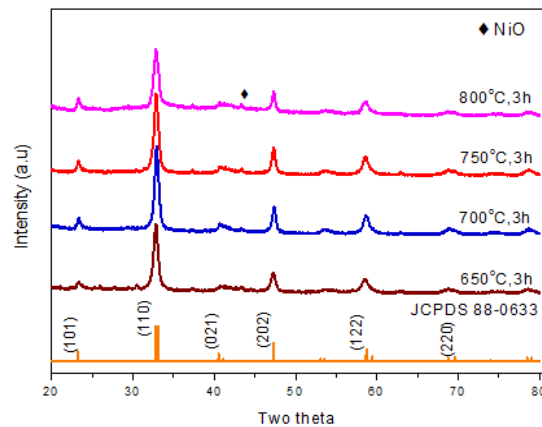


Figure 3: XRD patterns of calcined  $\text{LaNiO}_3$  powder of at different temperatures

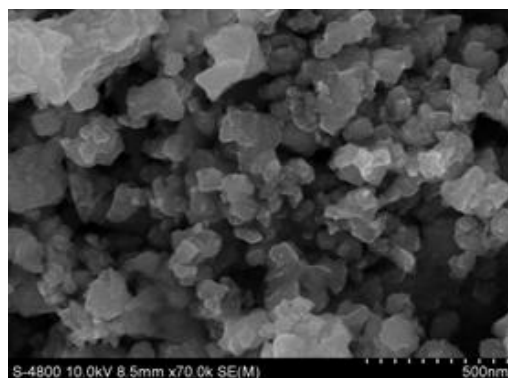


Figure 4: SEM image of the as synthesized product (calcined at 700 °C for 3 hours)

Fig. 4 shows microstructure of the  $\text{LaNiO}_3$  product which was calcined at 700 °C for 3 hours. One can see the homogeneously distorted cubic particles of sizes about 50–100 nm and their agglomerates.

#### Removal of 2-naphthol residues by the synthesized products

Fig. 5 shows typical removal yields of 2-naphthol from aqueous samples during sorption and – illumination times. Sorption onto the product's surface represented about 25% removal yield and visible-light catalytic process increased this removal yield up to about 99% after 4 hours illumination.



Fig.6 compares FT-IR spectra of the selected  $\text{LaNiO}_3$  product before and after its application in 2-naphthol removal experiments. Beside the typical absorption bands at wavenumbers around  $\sim 650 \text{ cm}^{-1}$ , representing vibrations of the M-O (M = La and Ni) bonds in its perovskite structure [2], spectra of the as synthesized  $\text{LaNiO}_3$  also shows more or less intense absorption bands around wavenumbers  $\sim 3430 \text{ cm}^{-1}$ ,  $1647 \text{ cm}^{-1}$ ,  $1493 \text{ cm}^{-1}$  and  $1420 \text{ cm}^{-1}$ , corresponding to the vibrations of bonds in hydroxylate, carboxylate, and carbonate groups, respectively [2, 7], which might be artifacts due to sorption of vapour components onto the sample surface. Adsorption of 2-naphthol resulted similar course of FT-IR spectra, except for the substantially more intense bands around  $1493 \text{ cm}^{-1}$  and  $1420 \text{ cm}^{-1}$  which are assigned to bond vibrations in the aromatic rings or carboxylates. These bands remain very intense after the photocatalytic experiments, indicating reactions on the  $\text{LaNiO}_3$  surface are substantially slower than the sorption step. Moreover, additional absorption bands around  $856 \text{ cm}^{-1}$  and  $721 \text{ cm}^{-1}$  corresponding to C-H and  $\gamma$ -OH [18] indicates that even the de-sorption of 2-naphthol transformation products were slow.

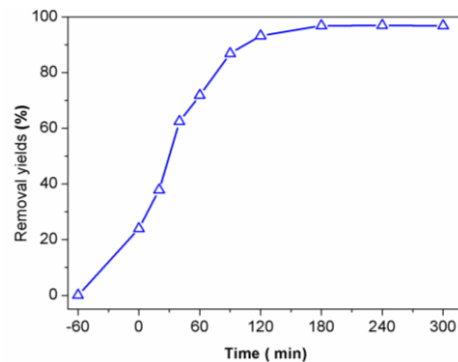


Figure 5: Removal yields of 10 ppm 2-naphthol using the prepared product

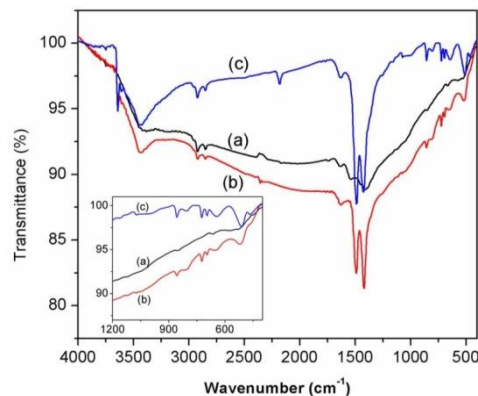


Figure 6: FT-IR spectra of the selected  $\text{LaNiO}_3$ : (a) as-synthesized, (b) after a sorption experiment for 30 minutes, and (c) after a photocatalytic experiment for 300 minutes

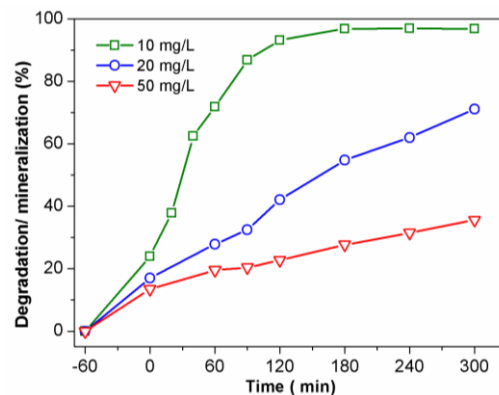


Figure 7: Effect of 2-naphthol initial conc. on its removal yields by the synthesized  $\text{LaNiO}_3$ .



Fig.7 demonstrates the effect of initial 2-naphthol concentration onto its removal yields by our synthesized  $\text{LaNiO}_3$ . The removal yields of 2-naphthol increased with decreasing its initial concentration as the number of activated sorption/photocatalytic sites on the  $\text{LaNiO}_3$  surface is limited. The removal kinetics could be described by rate equations of pseudo-first order reactions – Fig.8, which could also be explained by the constant number of catalytic sites on  $\text{LaNiO}_3$  surface.

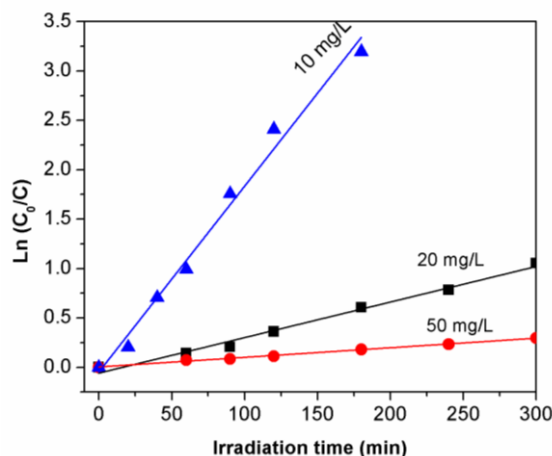


Figure 8: Kinetic fit of degradation of 2-naphthol in the presence of  $\text{LaNiO}_3$

Table 3 summarizes the calculated rate constants of the observed pseudo-first order reaction to remove 2-naphthol. They are all higher than value  $k = 0.016 \text{ min}^{-1}$  reported for  $\text{TiO}_2$  “PC-50” in the literature [11], *i.e.* the synthesized  $\text{LaNiO}_3$  could serve as powerful photocatalysts operating under visible lights illumination for treating 2-naphthol residues in water.

Table 3: The rate constant of the pseudo first order reaction

$C_0$ (ppm)	$k$ ( $\text{min}^{-1}$ )	$R^2$
10	$1.882 \times 10^{-2}$	0.986
20	$0.360 \times 10^{-2}$	0.987
50	$0.097 \times 10^{-2}$	0.995

In addition, the waste  $\text{LaNiO}_3$  could be regenerated up to 2 times, resulting in slightly decrease of 2-naphthol removal yields from 96.8 % for the first application to 86.5 % for the third one. It can be due to the fouling of catalyst and the loss after filtration process [20].

## Conclusion

Crystalline  $\text{LaNiO}_3$  was synthesized via a sol gel method using citric acid as oxidizing agent. The synthesis procedure was optimized and the as synthesized product proved to own the desired perovskite structure. Its photocatalytic activity to remove 2-naphthol residues (initial conc. 10–50 ppm) under visible lights illumination has been confirmed. Further investigation dealing with effects of typical components in surface water as well as identifying transformation products of 2-naphthol is in progress.

## Acknowledgement

This research was funded by the CARE-Rescif, under grant number Tc-KTHH-2016-07.

## References

- [1]. Fei L., Kai Y., Lou L.L., Su Z., Liu S. (2010). Theoretical and experimental study of La/Ni co-doped  $\text{SrTiO}_3$  photocatalyst, *Materials Science and Engineering B* 172:136–141
- [2]. Rida K., Peña M.A., Sastre E., Martínez-Arias A. (2012). Effect of calcination temperature on structural properties and catalytic activity in oxidation reactions of  $\text{LaNiO}_3$  perovskite prepared by Pechini method, *Journal of rare earths*, 30(3) 210



- [3]. Wang Y., Yang X., Lu L., Wang X. (2006). Experimental study on preparation of  $\text{LaMO}_3$  ( $M = \text{Fe, Co, Ni}$ ) nanocrystals and their catalytic activity, *Thermochimica Acta* 443, 225–230
- [4]. Wallin M., Cruise N., Klement U., (2004). Preparation of Mn, Fe and Co based perovskite catalysts using microemulsions, *Colloids and Surfaces A: Physicochem. Eng. Aspects* 238, 27–35
- [5]. E. García-López, G. Marci, F. Puleo, V. La Parola, L.F. Liotta, (2015).  $\text{La}_{1-x}\text{Sr}_x\text{Co}_{1-y}\text{Fe}_y\text{O}_{3-\delta}$  perovskites: Preparation, characterization and solar photocatalytic activity, *Applied Catalysis B: Environmental*, 178, 218–2254
- [6]. Fei D.Q., Hudaya T., Adesoji A. Adesina, Visible-light activated titania perovskite photocatalysts: Characterisation and initial activity studies, *Catalysis Communications* 6 (2005) 253–258.
- [7]. Tomohiro I., Yasuyuki S., Yuri M., Satoru W., (2016). Mechanochemically assisted synthesis and visible light photocatalytic properties of lanthanum nickel oxide nanoparticles, *Optik* 127, 9081–9087.
- [8]. Aman D., Zaki T., Mikhail S., Selim S.A. (2011). Synthesis of a perovskite  $\text{LaNiO}_3$  nanocatalyst at a low temperature using single reverse microemulsion, *Catalysis Today* 164, 209–213.
- [9]. Yuanyuan L., Shanshan Y., Wei W., Lihong X., Youwei Y. (2010). Sol-gel combustion synthesis and visible-light-driven photocatalytic property of perovskite  $\text{LaNiO}_3$ , *Journal of Alloys and Compounds* 491, 560–564.
- [10]. Peisong T., He S., Feng C., Jintian Y., Shengliang N. and Haifeng C. (2011). Visible-light Driven  $\text{LaNiO}_3$  Nanosized Photocatalysts Prepared by a Sol-gel Process, *Advanced Materials Research Vol. 279*, 83–87.
- [11]. Qourzal S., Barka N., Tamimi M., Assabbane A., Ait-Ichou Y. (2008). Photodegradation of 2-naphthol in water by artificial light illumination using  $\text{TiO}_2$  photocatalyst: Identification of intermediates and the reaction pathway, *Applied Catalysis A: General* 334, 386–393.
- [12]. Jie L., Chaoying Y., Peiqing Z., Gexin C. (2012). Comparative study of supported  $\text{CuO}_x$  and  $\text{MnO}_x$  catalysts for the catalytic wet air oxidation of  $\beta$ -naphthol, *Applied Surface Science*, 258, 9096–9102.
- [13]. Edvinas K., Dainius M., Martynas T., Dalia J. (2015). Decomposition of 2-naphthol in water using a non-thermal plasma reactor, *Chemical Engineering Journal*, 260, 188–198.
- [14]. Shuyan Z., Bin L., Juan W., Yanjie Y., (2010). Biodegradation of 2-naphthol and its metabolites by coupling *Aspergillus niger* with *Bacillus subtilis*, *Journal of Environmental Sciences*, 22(5) 669–674,
- [15]. Qourzal S., Barka N., Tamimi M., Assabbane A., (2009). Sol-gel synthesis of  $\text{TiO}_2\text{-SiO}_2$  photocatalyst for  $\beta$ -naphthol photodegradation, *Materials Science and Engineering C* 29, 1616–1620.
- [16]. Xiaohui S., Wenfei H., Zhanyu M., Yingying L., Xueyou S. (2013). A novel approach for removing 2-naphthol from wastewater using immobilized organo-bentonite, *Journal of Hazardous Materials* 252–253, 192–197
- [17]. Heidi E. H., (1993). Crystal Chemistry and Thermal Behavior in the  $\text{La}(\text{Cr,Ni})\text{O}_3$  Perovskite System, *J. Electrochem. Soc.*, 140(10).2889–2894.
- [18]. Sunxian W., Zeng X. P., Zuyang Z., Exciton-Free (2013). Nonsensitized Degradation of 2-Naphthol by Facet- Dependent  $\text{BiOCl}$  under Visible Light: Novel Evidence of Surface- State Photocatalysis, *ACS Appl. Mater. Interfaces*, 5 (23), 12380–12386.
- [19]. Neren O., Elc in S., (2008). Characterization and photocatalytic activity of  $\text{TiO}_2$  supported sepiolite catalysts, *Separation and Purification Technology* 62, 535–543.
- [20]. Ahmed K., Leghari S., Sajjad S. (2010). Comparative studies of operational parameters of degradation of azo dyes in visible light by highly efficient  $\text{WO}_3/\text{TiO}_2$  photocatalyst, *Journal of Hazardous Materials* 177, 781–791.

